Bulletin of Earth Sciences of Thailand

Mineral chemistry of biotite from granitic rocks in Prachuap Khiri Khan, southern Thailand: Implications for crystallization condition and petrogenesis

Montree Sirimongkonpun[1], Thirawat Tukpho[1], Alongkot Fanka[2,*]

[1] Department of Geology, Faculty of Science, Chulalongkorn University, Bangkok 10330, Thailand
[2]Applied Mineral and Petrology Special Task Force for Activating Research (AMP STAR), Department of Geology, Faculty of Science, Chulalongkorn University, Bangkok, 10330 Thailand
* Corresponding author e-mail: alongkot.f@chula.ac.th

Received: 23 May 2023
Revised: 05 Jul 2023
Accepted: 05 Jul 2023

Abstract

This study investigates the characteristics and mineral chemistry of biotite from porphyritic muscovite-biotite granite in the Prachuap Khiri Khan area, southern Thailand. The biotites in this granite exhibit distinctive features, including the presence of siderophyllite and Fe-biotite endmembers. The obtained mineral chemistry of biotite indicates that the granite's formation occurred in a collisional setting. The prevailing oxidizing conditions, as indicated by the nickel-nickel oxide to fayalite-magnetite-quartz buffer range, played a crucial role in shaping the chemical composition of the biotites. Furthermore, the analysis suggests the involvement of hydrous conditions during the granite's formation. Based on biotite geothermobarometry, the crystallization temperature of the biotite ranges from 631 to 719 °C, and crystallization pressure ranges from 2.73 to 4.05 kbar. These P-T conditions provide valuable insights into the thermal history and crystallization conditions of the granite. Additionally, the corresponding pressures are equivalent to an emplaced depth from 10.2 to 15.1 km of the granites in this area.

Keywords: Biotite geochemistry, Granite, Petrology, Geothermobarometry, Thailand

1. Introduction

Mineral chemistry of biotite is a widely used approach in igneous petrology for understanding the evolution of magmas and their associated rocks (Jacobs and Parry, 1976, 1979; Tang et al., 2019; Kazemi et al., 2022). Biotite, an common mineral in granitic rocks, is generally considered to be one of the last minerals to crystallize during the cooling of a magma (Bowen, 1922). As a result, it often contains important information regarding the chemical composition and conditions of formation of the rock.

The chemical compositions of biotite can provide information about the source of the magma, temperature and pressure conditions during crystallization, and the evolution of the magma. Biotite chemistry is suggested to indicate original composition of the granitic magma (Abdel-Rahman, 1994). Moreover, the oxygen fugacity (fO_2) of the magmatic system can be carried out by the Fe^{2+}-Fe^{3+}-Mg ratio of biotite (Wones and Eugster, 1965).

In the Prachuap Khiri Khan area, southern Thailand (Fig.1), there are extensive exposures of granitic rocks of porphyritic muscovite-biotite granite presenting the biotite as one of the typical assemblages in the rock

(Putthapiban, 1984; Cobbing et al., 1992; Charusiri et al., 1993).

Therefore, the objective of this study is to investigate mineral chemistry of biotite from granitic rocks in Prachuap Khiri Khan, southern Thailand to understand the magmatic processes, crystallization conditions, petrogenesis of granitic rocks in the Prachuap Khiri Khan, southern Thailand, and magmatism of granitic rocks in Thailand and Southeast Asia.

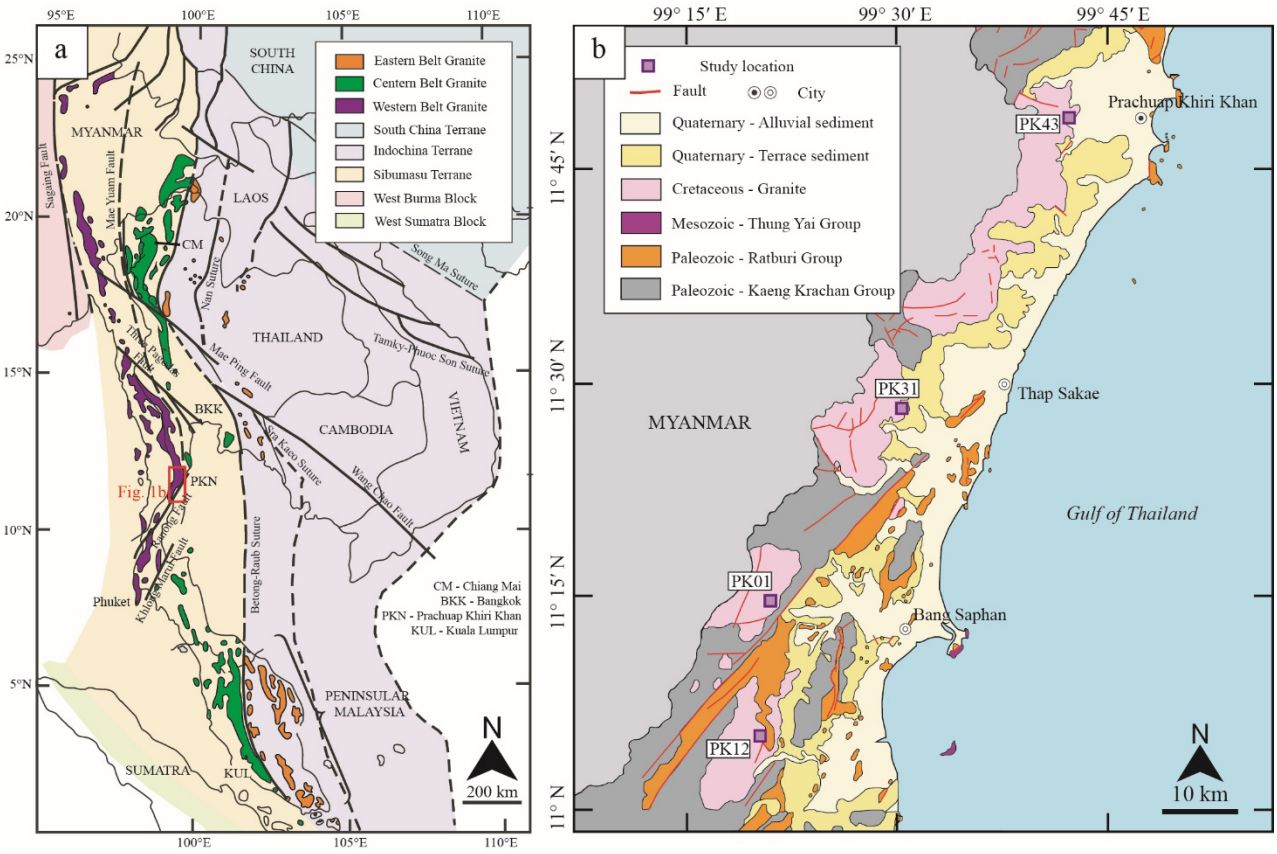

Figure 1 (a) Distribution of granitic rocks and tectonic terranes in Thailand and Southeast Asia (modified after Cobbing et al., 1992; Hutchison, 2014) and (b) Simplified geologic map of the study area (modified after Sudasna et al., 1976).

2. General geology

In the southern part of Thailand, specifically in the Prachuap Khiri Khan area (as illustrated in Fig. 1b), there are three primary types of rock units, namely Paleozoic sedimentary rocks, Mesozoic sedimentary rocks, and granitic rocks (Sudasna et al., 1976).

The Paleozoic sedimentary rocks are composed of two groups, namely the Kaeng Krachan and Ratburi Groups. The Kaeng Krachan Group predominantly consists of sandstone, pebbly mudstone, and shale, with NE-SW and NW-SE bedding trends (Piyasin, 1975; Chaodumrong et al., 2004; Chaodumrong et al., 2007). The Ratburi Group is dominated by limestone, characterized by massive and bedded limestone with fossils, interbedded with feldspathic and calcareous sandstone (Brown, 1951; Javanaphet and Dai, 1969). In addition, the Ratburi Group includes arkosic sandstone, and shale, characterized by massive and thick-bedded, fine to medium-grained sandstone interbedded with thin-bedded limestone in the

lower part together with NE-SW and NW-SE bedding trending (Bunopas, 1992; Chaodumrong et al., 2004; Chaodumrong et al., 2007). The Mesozoic sedimentary rocks are composed of reddish-brown shale, sandstone, and conglomerate, collectively known as the Thung Yai Group (Raksaskulwong, 2002). These non-marine deposits originate from the lower Middle Jurassic to Upper Cretaceous (Buffetaut et al., 1994; Teerarungsigul, 1999).

The granitic rocks in the area are Cretaceous granites, such as fine to coarse-grained biotite-muscovite granite, biotite granite, and tourmaline granite (Pongsapich et al., 1983; Charusiri et al., 1989; Charusiri et al., 1993; Watkinson et al., 2011; Sanematsu et al., 2015). These rocks were formed during collision between the West Burma terrane and the Sibumasu terrane around 100–60 million years ago (Charusiri et al., 1993; Searle et al., 2012; Ridd and Watkinson, 2013; Li et al., 2018; 2019). Figure 1a shows these granites from Eastern Belt Granite (EBG) in Indochina terrane, Central Belt Granite (CBG) and Western Belt Granite (WBG) in the Sibumasu Terrane.

3. Methodology

In this study, biotite was sampled from porphyritic muscovite-biotite granite in Prachuap Khiri Khan area, southern Thailand (Fig.1). The samples were prepared as polished thin sections and examined under a NIKON polarizing microscope at the Department of Geology, Faculty of Science, Chulalongkorn University, Thailand to identify their petrographic characteristics. The biotite chemistry was analyzed using an Electron Probe Microanalyzer (EPMA, model JEOL JXA-8100) at the Department of Geology, Faculty of Sciences, Chulalongkorn University. The EPMA was operated at a 15.0 kV accelerating voltage and a 15 nA sample current. Calibration standards in the form of pure oxide and mineral standards were used. The analytical results were obtained using the automatic ZAF correction method provided by JEOL. The Fe^{2+} and Fe^{3+} ratios and $\log fO_2$ of biotite were calculated by the method described by Li et al., (2020b). The analytical results of representative biotite chemistry are presented in Table 1.

4. Results

The porphyritic muscovite-biotite granite referred to the WBG of Thailand is prevalent throughout the western part of the study area. These rocks are commonly observed as large natural outcrops and stream-cut outcrops in the study area (Fig. 2).

These granites can be found in four different exposures in the study area (Fig. 1b). All granites in all exposures show similar petrological characteristics. The porphyritic muscovite-biotite granite in the study area is represented by porphyritic texture with prominent feldspar phenocrysts. These granites are composed of quartz (15 – 40%), K-feldspar (30 – 60%), plagioclase (5 – 25%), biotite (5 – 20%), muscovite (1 – 5%), and minor accessory minerals (1 – 2%), such as zircon, apatite, monazite, tourmaline, and ilmenite (Fig. 3). The porphyritic muscovite-biotite granite also exhibits various igneous textures, including myrmekitic texture of quartz and K-feldspar, poikilitic, and perthitic textures, as shown in Figure 3.

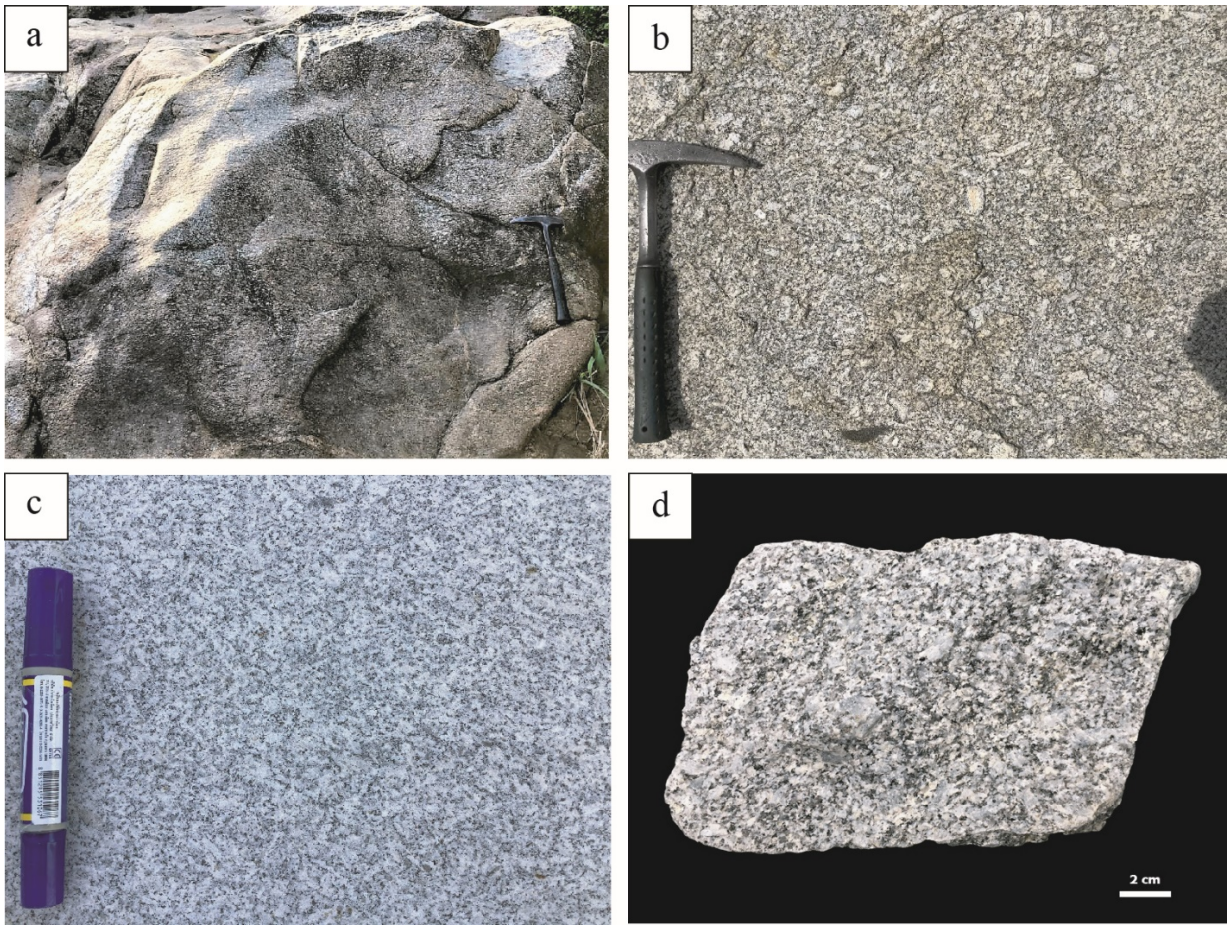

Figure 2 Representative outcrop exposures of porphyritic muscovite-biotite granite samples (a) PK01, (b) PK12, (c) PK31, and (d) PK43.

The mineral chemistry data obtained from EPMA analysis of biotite in the porphyritic muscovite-biotite granites are presented in Table 1. Table 1 provides information on the weight percentages of various components in biotite, including SiO_2 (32.02 – 33.95%), Al_2O_3 (16.34 – 18.90%), TiO_2 (2.54 – 4.53%), FeOt (24.75 – 25.99%), MnO (0.26 – 0.40%), Na_2O (0.05 – 0.17%), K_2O (9.27 – 9.73%), and MgO (5.33 – 6.80%).

The relationship between the mole fraction of magnesium (X_{Mg}) and the content of major oxides in biotite is depicted in Figure 4. The X_{Mg} value of biotite exhibits a positive correlation with the Al_2O_3 content while showing a negative correlation with the TiO_2 content. Moreover, the X_{Mg} value displays a scattered distribution pattern when compared to the SiO_2, MnO, Na_2O, and K_2O contents. These findings, along with the X_{Mg} value, indicate that these granites are similar to the characteristics of biotite in the granitic rocks in the WBG (Li et al., 2020a).

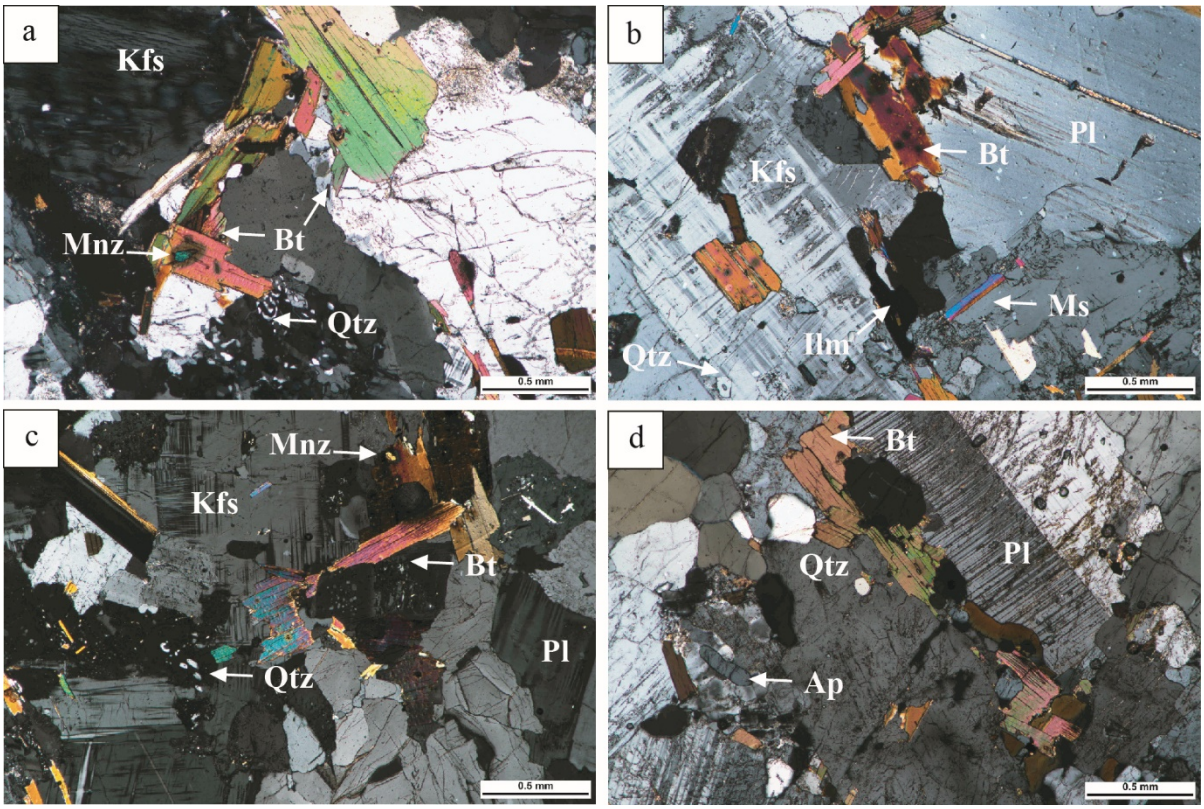

Figure 3 Photomicrograph of porphyritic muscovite-biotite granite samples (a) PK01, (b) PK12, (c) PK31, and (d) PK43. Abbreviations: Pl = plagioclase; Kfs = K-feldspar; Qtz = quartz; Bt = biotite; Ms = muscovite; Ap = apatite; Mnz = monazite; Ilm = ilmenite.

5. Discussion

5.1 Biotite classification

According to the classification scheme established by the International Mineralogical Association (IMA) for micas (Rieder et al., 1998), the biotite can be classified into four end-members: annite, phlogopite, siderophyllite, and eastonite. In the Mg/(Mg + Fe) vs. Al diagram (Fig. 5a) (Rieder et al., 1998), the biotite closely resembles the siderophyllite end-member, suggesting a considerable iron (Fe) enrichment. According to nomenclature for trioctahedral mica classification of Foster (1960), all the biotite samples fall within the Fe-biotite field (Fig. 5b). The TiO_2 content is commonly utilized as a discriminating parameter to characterize magmatic biotite, primarily due to its tendency to crystallize under higher temperatures compared to other types of biotite (Patiño Douce and Harris, 1998). This discernment further supports the hypothesis that the examined biotite samples were formed by a magmatic origin substantiated by their occurrence as phenocrysts intergrown with other magmatic minerals. Plotting the biotite samples on the TiO_2-FeOt+MnO-MgO ternary diagram (Nachit et al., 2005), the biotites are fitted in primary magmatic biotite field within the expected range for biotite in common granitic rocks (Fig. 5c). These observations in all mentioned diagrams are consistent with the findings of previous research on the biotite composition in granite formations of WBG in southern Myanmar (Li et al., 2020a).

Table 1 Representative EPMA analyses of biotite in granitic rocks from Prachuap Khiri Khan, southern Thailand. Abbreviations: T. = tetrahedral, O. = octahedral, and A. = interlayer.

Sample No	PK01			PK12			PK31			PK43		
Rock name	Porphyritic muscovite-biotite granite			Porphyritic muscovite-biotite granite			Porphyritic muscovite-biotite granite			Porphyritic muscovite-biotite granite		
Latitude	11.247156			11.083913			11.473292			11.796429		
Longtitude	99.337862			99.339637			99.497184			99.700065		
Analysis No.	bt4-2	bt6-2	bt7-2	bt1-1	bt7-1	bt8-2	bt2-1	bt4-1	bt9-1	bt2-2	bt7-2	bt9-2
SiO_2	33.08	33.15	32.02	33.28	33.23	33.06	33.57	33.95	33.35	33.51	33.17	33.19
Al_2O_3	17.39	17.32	17.53	18.90	18.41	18.54	18.70	17.99	18.06	17.41	16.49	16.34
TiO_2	4.53	4.38	3.85	2.60	2.87	2.69	2.54	2.62	2.68	3.71	4.37	4.36
FeOt	25.01	25.36	24.83	25.40	25.24	25.08	25.77	24.75	24.37	25.32	25.99	25.10
MnO	0.37	0.40	0.40	0.39	0.40	0.36	0.33	0.36	0.34	0.28	0.34	0.26
MgO	5.54	5.85	5.67	6.80	6.65	6.56	5.88	6.29	6.17	5.79	5.54	5.33
CaO	0.00	0.00	0.00	0.00	0.00	0.00	0.00	0.00	0.00	0.00	0.00	0.00
Na_2O	0.05	0.12	0.17	0.11	0.07	0.09	0.05	0.08	0.04	0.13	0.08	0.07
K_2O	9.48	9.73	9.55	9.57	9.63	9.65	9.39	9.48	9.30	9.50	9.52	9.24
Total	**95.45**	**96.30**	**94.02**	**97.04**	**96.50**	**96.02**	**96.24**	**95.52**	**94.30**	**95.65**	**95.51**	**93.88**
O (11)												
T. Si	2.66	2.66	2.62	2.61	2.62	2.62	2.64	2.68	2.66	2.68	2.68	2.70
T. Al	1.25	1.25	1.29	1.30	1.28	1.29	1.25	1.20	1.23	1.21	1.19	1.16
T. Fe^{3+}	0.08	0.09	0.09	0.09	0.10	0.10	0.11	0.12	0.11	0.11	0.13	0.14
Total T.	**4.00**	**4.00**	**4.00**	**4.00**	**4.00**	**4.00**	**4.00**	**4.00**	**4.00**	**4.00**	**4.00**	**4.00**
M. Al	0.40	0.38	0.41	0.44	0.43	0.45	0.49	0.47	0.47	0.43	0.38	0.41
M. Mg	0.73	0.75	0.77	0.81	0.81	0.81	0.72	0.78	0.79	0.74	0.73	0.73
M. Fe^{2+}	1.51	1.51	1.50	1.45	1.46	1.47	1.49	1.43	1.44	1.49	1.52	1.49
M. Fe^{3+}	0.09	0.10	0.11	0.12	0.11	0.10	0.10	0.08	0.08	0.09	0.10	0.08
M. Ti	0.26	0.25	0.23	0.15	0.16	0.15	0.15	0.15	0.16	0.21	0.25	0.26
M. Mn	0.03	0.03	0.03	0.03	0.03	0.02	0.02	0.02	0.02	0.02	0.02	0.02
Total M.	**3.01**	**3.02**	**3.04**	**3.00**	**3.00**	**3.00**	**2.97**	**2.95**	**2.96**	**2.98**	**3.01**	**2.98**
A. K	0.96	0.98	0.98	0.94	0.96	0.96	0.94	0.95	0.94	0.95	0.97	0.95
A. Na	0.01	0.02	0.03	0.02	0.01	0.01	0.01	0.01	0.01	0.02	0.01	0.01
A. Ca	0.00	0.00	0.00	0.00	0.00	0.00	0.00	0.00	0.00	0.00	0.00	0.00
Total A.	**0.97**	**0.99**	**1.00**	**0.96**	**0.97**	**0.97**	**0.94**	**0.96**	**0.95**	**0.97**	**0.98**	**0.96**
X_{Mg}	0.33	0.33	0.34	0.36	0.36	0.36	0.33	0.35	0.35	0.33	0.33	0.32
Ti (pfu)	0.52	0.50	0.45	0.29	0.33	0.31	0.29	0.31	0.32	0.43	0.50	0.51
Alt (pfu)	3.30	3.27	3.38	3.49	3.42	3.46	3.47	3.35	3.40	3.28	3.14	3.06
T (°C)	719	714	701	634	653	644	631	643	649	693	715	716
P (kbar)	3.47	3.38	3.72	4.05	3.85	3.96	3.99	3.62	3.78	3.40	2.98	2.73
h (km)	13.0	12.6	13.9	15.1	14.4	14.8	14.9	13.5	14.1	12.7	11.1	10.2

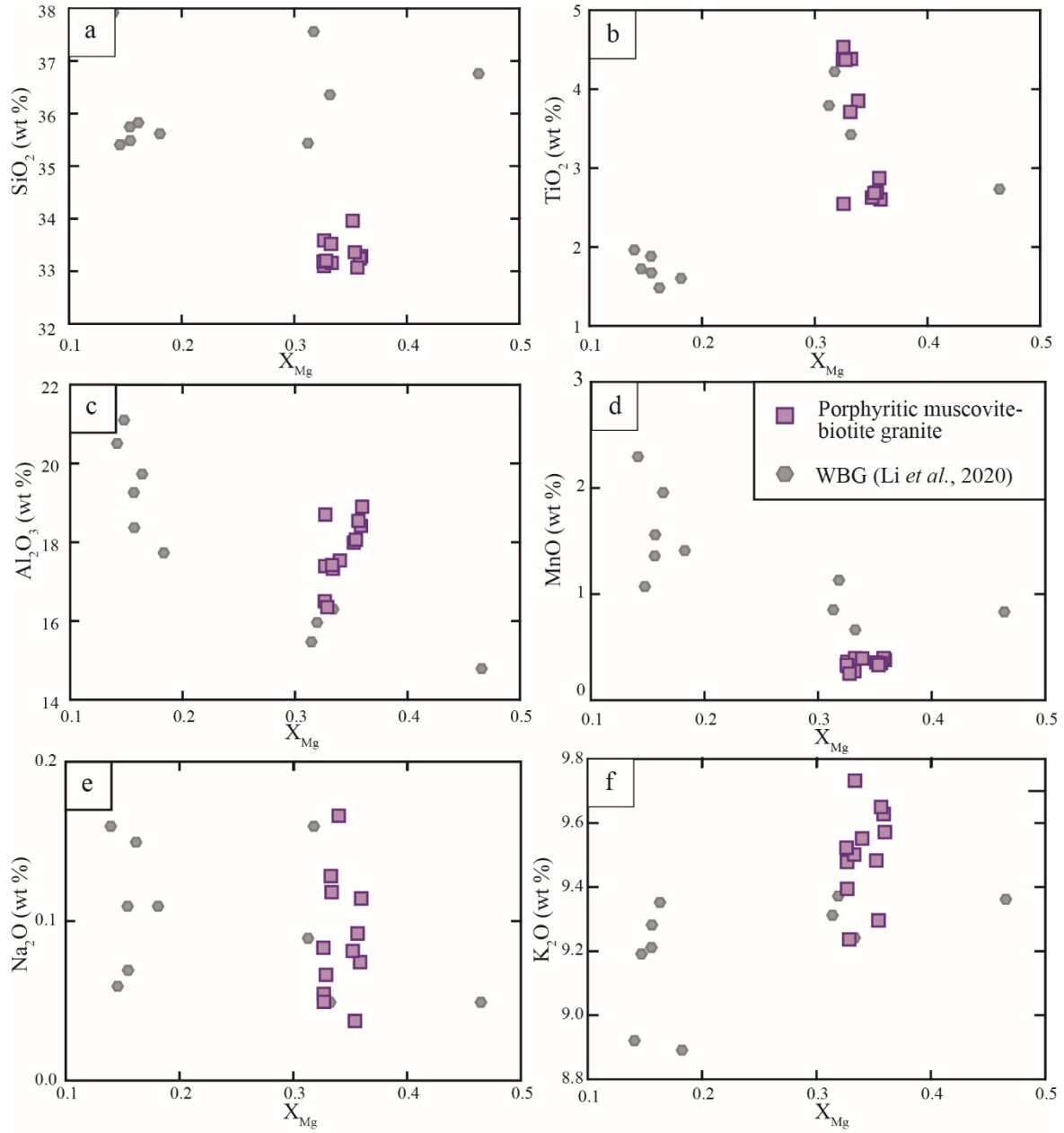

Figure 4 Binary plots for the biotite of porphyritic muscovite-biotite granite in Prachuap Khiri Khan area. (a) SiO_2 vs. X_{Mg}; (b) TiO_2 vs. X_{Mg}; (c) Al_2O_3 vs. X_{Mg}; (d) MnO vs. X_{Mg}; (e) Na_2O vs. X_{Mg}; and (f) K_2O vs. X_{Mg}.

5.2 Crystallization conditions

5.2.1 Temperature, pressure, and magma source

As the titanium (Ti) content in biotite is influenced by temperature, the Ti-content in biotite has been used for Ti-in biotite geothermometer to estimate the crystallization temperature (Stussi and Cuney, 1996; Patiño Douce and Harris, 1998). In this study, the biotite geothermometer suggested by Henry et al. (2005) was employed to estimate the crystallization temperature of the granitic rocks. The calculation utilized the equation: T = {[ln (Ti) +

$2.3594+1.7283(X_{Mg})^3]/4.6482\ x10^{-9}\}^{0.333}$, where T represents the temperature in degrees Celsius, Ti denotes the number of atoms per formula unit (apfu) based on 22 oxygen atoms, and X_{Mg} refers to the ratio of magnesium (Mg) to the sum of magnesium and iron (Fe) (Table 1). The calculated temperature results range from 631 to 719 °C.

Given that the biotite is present in the porphyritic muscovite-biotite granite, crystallization pressure and depth can provide insights into the intrusion condition of the granitic rocks. In terms of the crystallization pressure of biotite, the biotite geobarometer of Uchida et al. (2007) was employed by using the calibration equation P (±0.33 kbar) = 3.03 x Alt – 6.53, where Alt represents the total aluminum (Al) content in biotite assuming 22 oxygen atoms. The calculated crystallization pressures of the biotites range from 2.73 to 4.05 kbar, corresponding to emplacement depths of approximately 10.2–15.1 km. These results are consistent with the demonstrated crystallization pressure-temperature (P-T) conditions observed in granitic rocks by Chi and Reed (2008). The estimated intrusion depths are indicative of the crustal level, aligning with the previously reported granitic seat proposed by Tewari et al. (2018).

The significant role of biotite chemistry in elucidating the petrogenesis of rocks has been provided by several researchers e.g., Wones and Eugster (1965), and Zhao et al. (2015). In the case of the biotites from porphyritic muscovite-biotite granite, the plots fall within the field of peraluminous collision magmatism related to S-type granite affinity on the MgO-FeOt-Al2O3 ternary diagrams (Abdel-Rahman, 1994) (Figs. 6a and 6b).

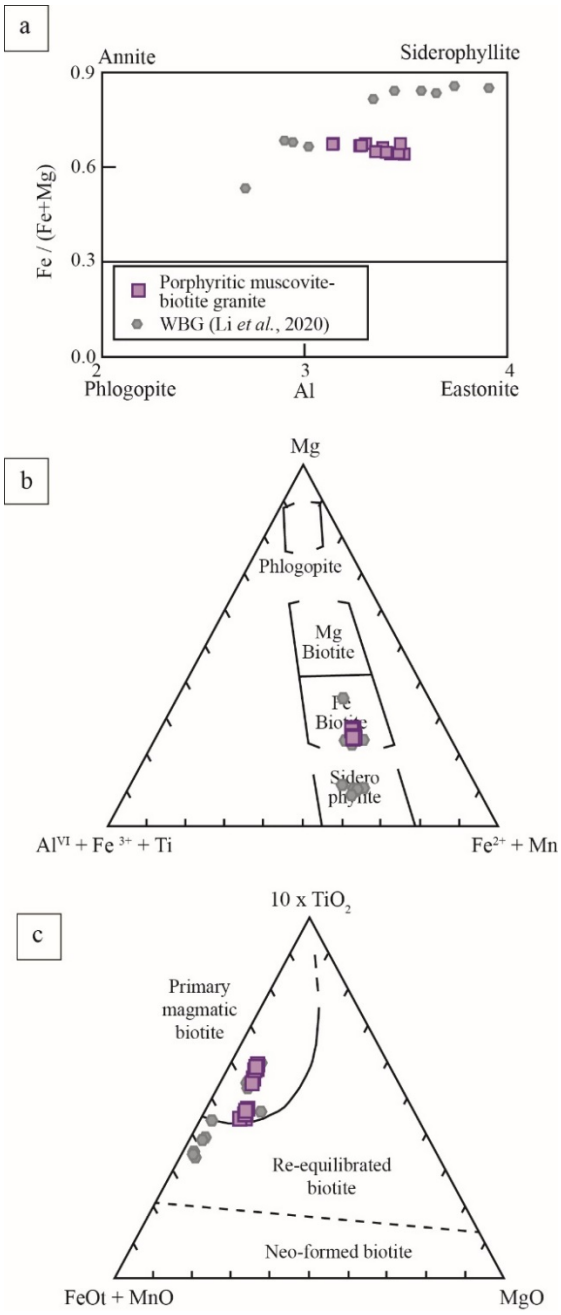

Figure 5 Plots of mineral chemistry for (a) feldspar (after Smith and Brown, 1974), (b) biotite (after Morimoto et al., 1988), (c) biotite classification (after Foster, 1960), and (d) $10xTiO_2$-FeOt+MnO-MgO ternary plots (after Nachit et al., 2005).

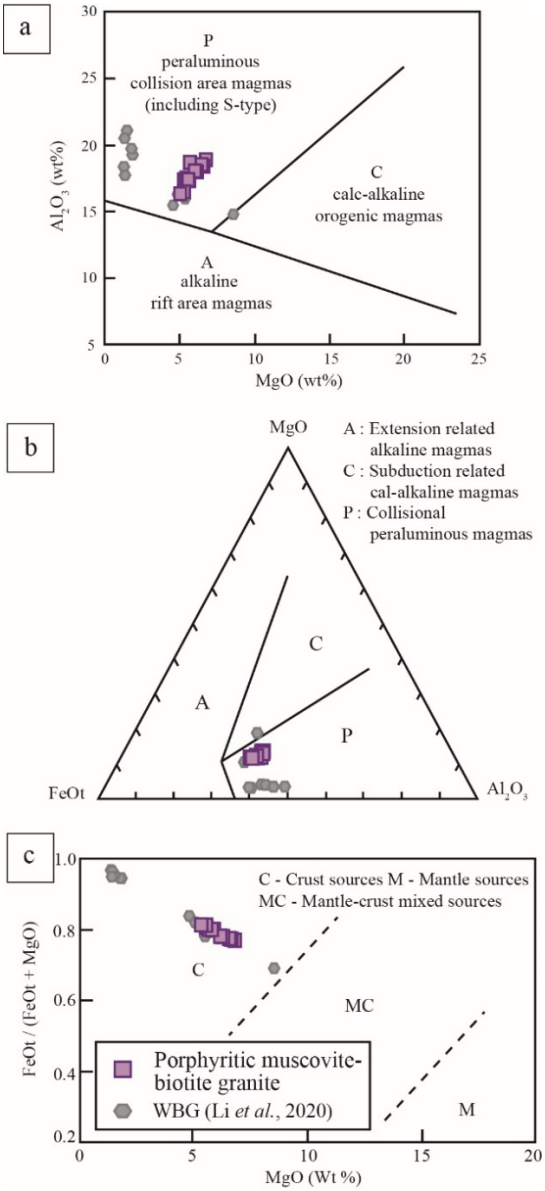

Figure 6 (a) Plots of biotite composition in the MgO vs. Al_2O_3 diagram (after Abdel-Rahman, 1994), (b) the FeOt-MgO-Al_2O_3 ternary diagram (after Abdel-Rahman, 1994), and (c) the MgO and FeOt/(FeOt+MgO) diagram (after Zhou, 1986).

These findings are consistent with the compositional characteristics of those granitic rocks from southern Myanmar (Li et al., 2020a). It is well-established that S-type granites commonly form in collision-related geological settings (Chappell and White, 1974). Therefore, these observations further support the previous suggestions that the WGB under investigation originated during the collision of the Sibumasu and West Burma terranes (Charusiri et al., 1993; Searle et al., 2012; Ridd and Watkinson, 2013; Li et al., 2018; Li et al., 2019). Furthermore, in the plots of MgO vs. FeO/(FeO + MgO) diagram (Zhou, 1986) (Fig. 6c), all biotites are clearly plotted within the field of crustal source. This result indicates that the porphyritic muscovite-biotite granite originated from a magma with the crustal source, which is further supported by the calculated intrusion depths discussed in the section of crystallization conditions, reflecting a close relationship with the crustal level.

5.2.2 Oxygen fugacity

The Fe^{2+}, Fe^{3+}, and Mg contents within biotite minerals have been utilized to estimate the oxygen fugacity (fO_2) of associated magmas and fluids, as documented by Wones and Eugster (1965). The ternary diagram (Fig. 7a) (Wones and Eugster, 1965; Buda et al., 2004) was used to plot the Fe^{2+}-Fe^{3+}-Mg composition of various samples. Notably, all the analyzed samples fell within the region bounded by the nickel-nickel oxide (NNO) and fayalite-magnetite-quartz (FMQ; Fe_2SiO_4- Fe_3O_4-SiO_2) fields on the diagram. This study result implies that these samples were formed within an oxidizing environment and can be classified as ilmenite-series granites. Additional evidence supporting this assertion arises from the presence of ilmenite in the porphyritic muscovite-biotite granite. Consequently, it can be inferred that the formation of biotites in the granitic rocks of the Prachuap Khiri Khan area occurred under oxidizing conditions. The mineral chemistry of biotite in this study is comparable to the WBG in other areas (Li et al., 2020a).

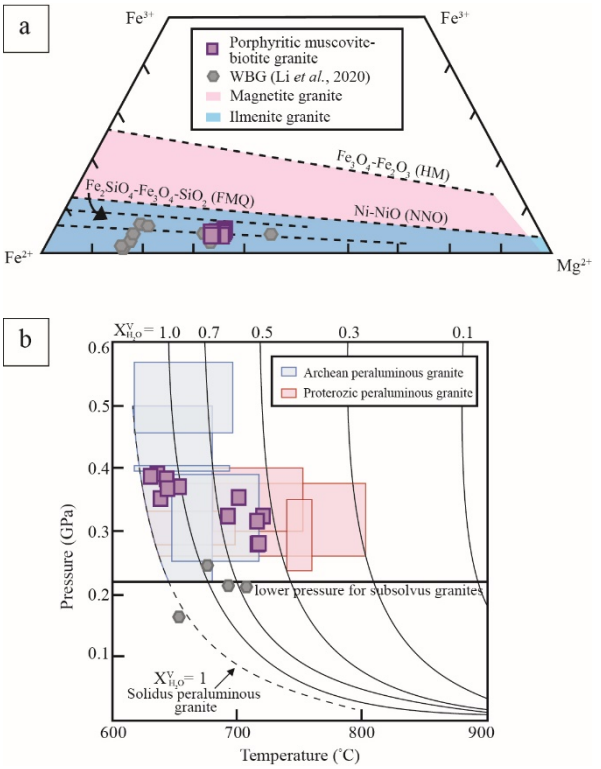

Figure 7 (a) Ternary Fe^{3+}-Fe^{2+}-Mg plot for the Prachuap Khiri Khan biotite (modified after Wones and Eugster, 1965; Buda et al., 2004), and (b) Plot of estimated T and P diagram for inferred crystallization conditions (after Bucholz et al., 2018).

Furthermore, the relationship between estimated temperature and pressure (Fig. 7b) (Bucholz et al., 2018) indicates that the experimentally controlled mole fraction of H_2O in the coexisting vapor phase (X_{H2O}^{V}) ranges from approximately 1 to 0.5. The results imply that these samples were formed within a hydrous environment. This range well aligns with the characteristics of Archean and Proterozoic peraluminous granites (Anderson and Thomas, 1985; Percival et al., 1985; Campion et al., 1986; Anderson and Bender, 1989; Feng and Kerrich, 1990; Helms and Labotka, 1991; Nabelek et al., 1992; Mulja et al., 1995; Parkinson and Arculus, 1999).

6. Conclusion

1. Mineral chemistry of biotite from the porphyritic muscovite-biotite granite in Prachuap Khiri Khan area can be classified as siderophyllite and Fe biotite endmembers.

2. Mineral chemistry of biotite shows that the granitic rocks were emplaced in the collision-related setting, under oxidizing conditions (the NNO to FMQ buffers), hydrous condition, at temperature ranging 631 to 719 °C, pressure ranging 2.73 to 4.05 kbar, and emplacement depth from 10.2 to 15.1 km.

Acknowledgements

The authors are grateful for the research facilities and analytical techniques provided by the Department of Geology, Faculty of Science, Chulalongkorn University, Thailand. The Development and Promotion of Science and Technology Talents Project (DPST) sponsored the first author for his MSc study. This work (Grant No. RGNS 64-022) was supported by Office of the Permanent Secretary, Ministry of Higher Education, Science, Research and Innovation (OPS MHESI), Thailand Science Research and Innovation (TSRI) and Chulalongkorn University.

References

Abdel-Rahman, A.M. 1994. Nature of biotites from alkaline, calc-alkaline and peraluminous magmas. *Journal of Petrology, 35*, 525-541.

Anderson, J.L. & Bender, E.E. 1989. Nature and origin of Proterozoic A-type granitic magmatism in the southwestern United States of America. *Lithos,* 23, 19-52.

Anderson, J.L. & Thomas, W.M. 1985. Proterozoic anorogenic two-mica granites:

Silver Plume and St. Vrain batholiths of Colorado. *Geology,* 13, 177-180.

Bowen, N. 1922. The reaction principle in petrogenesis. *The Journal of Geology,* 30, 177-198.

Brown, G.F. 1951. Geologic reconnaissance of the mineral deposits of Thailand. US Government Printing Office, the United States.

Bucholz, C.E., Stolper, E.M., Eiler, J.M. & Breaks, F.W. 2018. A comparison of oxygen fugacities of strongly peraluminous granites across the Archean–Proterozoic boundary. *Journal of Petrology,* 59, 2123-2156.

Buda, G., Koller, F., Kovács, J. & Ulrych, J. 2004. Compositional variation of biotite from Variscan granitoids in Central Europe: a statistical evaluation. *Acta Mineralogica-Petrographica,* 45, 21-37.

Buffetaut, E., Raksaskulwong, L., Suteethorn, V. & Tong, H. 1994. First post-Triassic temnospondyl amphibians from the Shan-Thai block: intercentra from the Jurassic of peninsular Thailand. *Geological Magazine,* 131, 837-839.

Bunopas, S. 1992. Regional stratigraphic correlation in Thailand, Proceedings of a National Conference on Geologic Resources of Thailand: Potential for Future Development, Bangkok, Thailand.

Campion, M., Perkins, D. & Roob, C. 1986. Contrasting contact zones between the English River Subprovince (ERSP) of Ontario–Manitoba and greenstone belts to the north and south. *Geological Society of America, Abstracts with Program*, 556.

Chaodumrong, P., Assavapatchara, S. & Jongautchariyakul, S. 2004. *Comparative research on Permian strata and fauna between West Yunnan and West Thailand.* Bangkok, Thailand.

Chaodumrong, P., Wang, X. & Shen, S. 2007. Permian lithostratigraphy of the Shan–Thai Terrane in Thailand: revision of the Kaeng Krachan and Ratburi groups, GEOTHAI'07 International Conference on Geology of Thailand: Towards Sustainable Development and Sufficiency Economy, Bangkok, 21-22.

Chappell, B.W. & White, A.J.R. 1974. Two contrasting granite types. Pacific *Geology,* 8, 173174.

Charusiri, P., Clark, A.H. & Farrar, E. 1989. *Miocene (Oligocene) Event in Thailand: evidences from $^{40}Ar/^{39}Ar$ and K-Ar geochronology.* The Annual Technical Meeting, 245-262. Department of Mineral Resources, Bangkok, Thailand.

Charusiri, P., Clark, A.H., Farrar, E., Archibald, D. & Charusiri, B. 1993. Granite belts in Thailand: evidence from the $^{40}Ar/^{39}Ar$ geochronological and geological synthesis. *Journal of Southeastern Asian Earth Sciences,* 8, 127-136.

Chi, W.C. & Reed, D.L. 2008. Evolution of shallow, crustal thermal structure from subduction to collision: An example from Taiwan. *Geological Society of America Bulletin,* 120, 679-690.

Cobbing, E.J., Pitfield, P., Darbyshire, D. & Mallick, D. 1992. The granites of the Southeast Asian Tin Belt. *Overseas Memoirs of the British Geological Survey, London,* 10, p. 388.

Feng, R. & Kerrich, R. 1990. Geobarometry, differential block movements, and crustal, structure of the southwestern Abitibi greenstone belt, Canada. *Geology,* 18, 870–873.

Foster, M.D. 1960. *Interpretation of the Composition of Triocta-hedral Micas*, Geological Survey Professional Paper 354–B, pp 49.

Helms, T.S. & Labotka, T.C. 1991. Petrogenesis of Early Proterozoic pelitic schists of the southern Black Hills, South Dakota: Constraints on regional low-pressure metamorphism. *Geological Society of America Bulletin,* 103, 1324-1334.

Henry, D., Guidotti, C. & Thomson, J. 2005. The Ti-saturation surface for low-to-medium pressure metapelitic biotites: implications for geothermometry and Ti-substitution Mechanism. *American Mineralogist,* 90, 316-328.

Hutchison, C.S. 2014. Tectonic evolution of Southeast Asia. *Bulletin of the Geological Society of Malaysia,* 60, 1-18.

Jacobs, D.C. & Parry, W.T. 1976. A comparison of the geochemistry of biotite from some Basin and Range stocks. *Economic Geology,* 71, 1029-1035.

Jacobs, D.C. & Parry, W.T. 1979. Geochemistry of biotite in the Santa Rita porphyry copper deposit, New Mexico. *Economic Geology,* 74, 860-887.

Javanaphet, J.C. & Dai, S.T.P. 1969. Geological map of Thailand: scale 1: 1,000.000. Department of Mineral Resources, Bangkok.

Kazemi, K., Modabberi, S. Xiao, Y., Sarjoughian, F. & Kananian, A. 2022. Geochronology, whole-rock geochemistry, SrNd isotopes, and biotite chemistry of the Deh-Bala intrusive rocks, Central Urumieh-Dokhtar Magmatic Arc (Iran): Implications for magmatic processes and copper mineralization. *Lithos,* 408-409, 106544.

Li, H., Myint, A.Z., Yonezu, K., Watanabe, K., Algeo, T.J. & Wu, J.H. 2018. Geochemistry and U–Pb geochronology of the Wagone and Hermyingyi A-type granites, southern Myanmar: implications for tectonic setting, magma evolution and Sn–W mineralization. *Ore Geology Reviews,* 95, 575-592.

Li, J.X., Fan, W.M., Zhang, L.Y., Ding, L., Yue, Y.H., Xie, J., Cai, F.-L., Quan, Q.-Y. & Sein, K. 2020a. Biotite geochemistry deciphers magma evolution of Sn-bearing granite, southern Myanmar. *Ore Geology Reviews,* 121.

Li, J.X., Fan, W.M., Zhang, L.Y., Evans, N.J., Sun, Y.L., Ding, L., Guan, Q.Y., Peng, T.P., Cai, F.L. & Sein, K. 2019. Geochronology, geochemistry, and Sr–Nd–Hf isotopic compositions of Late Cretaceous–Eocene granites in southern Myanmar: Petrogenetic, tectonic, and metallogenic implications. *Ore Geology Reviews,* 112, 103031.

Li, X., Zhang, C., Behrens, H. & Holtz, F. 2020b. Calculating biotite formula fromelectron microprobe analysis data using a machine learning method based on principal components regression. *Lithos,* 356, 105371.

Morimoto, N., Fabries, J., Ferguson, A.K., Ginzburg, I.V., Ross, M., Seifert, F.A., Zussman, J., Aoki, K. & Gottardi, G. 1988. Nomenclature of pyroxene. *American Mineralogist,* 73, 1123-1133.

Mulja, T., Williams-Jones, A.E., Wood, S.A. & Boily, M. 1995. The rare-element-enriched monzogranite-pegmatite-quartz vein systems in the Preissac-Lacorne Batholith, Quebec; I, Geology and mineralogy. *The Canadian Mineralogist,* 33, 793-815.

Nabelek, P.I., Russ-Nabelek, C. & Denison, J. 1992. The generation and crystallization conditions of the Proterozoic Harney Peak leucogranite, Black Hills, South Dakota, USA: petrologic and geochemical constraints. *Contributions to Mineralogy and Petrology,* 110, 173-191.

Nachit, H., Ibhi, A. & Ohoud, M.B. 2005. Discrimination between primary magmatic biotites, reequilibrated biotites and neoformed biotites. *Comptes Rendus Geoscience,* 337, 1415-1420.

Parkinson, I.J. & Arculus, R.J. 1999. The redox state of subduction zones: insights from arc-peridotites. *Chemical Geology,* 160, 409-423.

Patiño Douce, A.E. & Harris, N. 1998. Experimental constraints on Himalayan anatexis. *Journal of petrology,* 39, 689-710.

Percival, J.A., Stern, R.A. & Digel, M.R. 1985. Regional geological synthesis of western Superior Province, Ontario. G*eological Survey of Canada Paper,* 85, 385-397.

Piyasin, S. 1975. Stratigraphy and sedimentology of the Kaeng Krachan Group (Carboniferous), *Proceedings of the Conference on Geology of Thailand, 1975.* Department of Geological Sciences, Chiang Mai University, Thailand, 25-36.

Pongsapich, W., Pisutha-Arnond, V. & Charusiri, P. 1983. Reviews of felsic plutonic rocks of Thailand. Proceedings on the Workshop on Stratigraphic Correlation of Thailand and Malaysia, 8-10 September 1983. Haad Yai, Thailand, 213-232.

Putthapiban, P., 1984. *Geochemistry, geochronology and tin mineralization of Phuket granites, Phuket, Thailand.* Ph.D. thesis, La Trobe University Victoria, Melbourne, Victoria, Australia, 421.

Raksaskulwong, L. 2002. *Thung Yai Group: Jurassic-Cretaceous transition and continental deposits in Southern Thailand.* Geological Survey Division, Department of Mineral Resources, Report 260/2545 (in Thai), 1-49.

Ridd, M.F. & Watkinson, I. 2013. The Phuket-Slate Belt terrane: tectonic evolution and strike-slip emplacement of a major terrane on the Sundaland margin of Thailand and Myanmar. *Proceedings of the Geologists' Association,* 124, 994-1010.

Rieder, M., Cavazzini, G., D'yakonov, Y.S., Frank-Kamenetskii, V.A., Gottardi, G., Guggenheim, S., Koval, P.W., Mueller, G., Neiva, A.M. & Radoslovich, E.W. 1998. Nomenclature of the micas. *Clays and clay mineral,s* 46, 586-595.

Sanematsu, K., Kon, Y. & Imai, A. 2015. Influence of phosphate on mobility and adsorption of REEs during weathering of granites in Thailand. *Journal of Asian Earth Scieces* 111, 14-30.

Searle, M.P., Whitehouse, M.J., Robb, L.J., Ghani, A.A., Hutchison, C.S., Sone, M., Ng, S.W.P., Roselee, M.H., Chung, S.L. & Oliver, G.J.H. 2012. Tectonic evolution of the Sibumasu–Indochina terrane collision zone in Thailand and Malaysia: constraints from new U–Pb zircon chronology of SE Asian tin granitoids. *Journal of the Geological Society,* 169, 489-500.

Smith, J.V. & Brown, W.L. 1974. Feldspar minerals. Springer-Verlag: Germany.

Stussi, J. & Cuney, M. 1996. Nature of biotites from alkaline, calc-alkaline and peraluminous magmas by Abdel-Fattah M. Abdel-Rahman: a comment. *Journal of Petrology,* 37, 1025-1029.

Sudasna, P., Pitakpaivan, K., Silpalit, M., Meesook, A., Lovacharasupaphon, S. & Chaodumrong, P. 1976. Geological map of Thailand 1:250,000. NC 47-3, Prachuap Khiri Khan. Department of Mineral Resources, Thailand.

Tang, P., Tang, J.X., Lin, B., Wang, L.Q., Zheng, W.B., Leng, Q.F., Gao, X., Zhang, Z.B. & Tang, X.Q. 2019. Mineral chemistry of magmatic and hydrothermal biotites from the Bangpu porphyry Mo (Cu) deposit, Tibet. *Ore Geology Reviews,* 115, 103122.

Teerarungsigul, N. 1999. Lithostratigraphy of non-marine mesozoic rocks: Thung Yai-Khlong Thom areas in southern part of Thailand. Msc. thesis, Chulalongkorn University, Thailand.

Tewari, H.C., Rajendra Prasad, B. & Kumar, P. 2018. Global and Indian scenario of crustal thickness. *Structure and Tectonics of the Indian Continental Crust and Its Adjoining Region*, 211-224.

Uchida, E., Endo, S. & Makino, M. 2007. Relationship between solidification depth of granitic rocks and formation of hydrothermal ore deposits. *Resource Geology,* 57, 47-56.

Watkinson, I., Elders, C., Batt, G., Jourdan, F., Hall, R. & McNaughton, N.J. 2011. The timing of strike-slip shear along the Ranong and Khlong Marui faults, Thailand. *Journal of Geophysical Research: Solid Earth,* 116, 1-26.

Wones, D.R. & Eugster, H.P. 1965. Stability of biotite: experiment, theory, and application. *American Mineralogist,* 50, 1228-1272.

Zhao, X., Yang, Z., Zheng, Y., Liu, Y., Tian, S. & Fu, Q. 2015. Geology and genesis of the post-collisional porphyry–skarn deposit at Bangpu, Tibet. *Ore Geology Reviews,* 70, 486-509.

Zhou, Z.X. 1986. The origin of intrusive mass in Fengshandong, Hubei province. *Acta Petrologica Sinica,* 2, 59-70.